CMS TN/93-111
15 October 1993

RPC Based CMS Muon Trigger
PROGRESS REPORT

H. Czyrkowski, R. Dąbrowski, W. Dominik, M. Konecki, J. Królikowski,
M. Lewandowski, Z. Mazur, P. Musiał, L. Ropelewski and K. Sułowski
Institute of Experimental Physics, Warsaw University, Poland

M. Górski and M. Szeptycka
Institute for Nuclear Studies, Warsaw, Poland

I. Kudła and G. Wrochna
CERN, Geneva, Switzerland
on leave of absence from Institute of Experimental Physics, Warsaw University, Poland

Contents

1 Introduction

Triggering is a crucial point at high luminosity machines like LHC. Small $\sigma \cdot BR$ values force the p_t threshold to be as low as a few GeV. In this region inclusive rates of prompt muons and those from π and K decays are of the order of 1-10 kHz. This is about the limit of capability of the CMS event filter processor farm in the first staging phase. Thus, the tradeoff between acceptance for interesting channels and overall trigger rate requires precise tuning of the trigger thresholds and steep efficiency curves.

2 Physics goals

2.1 Low luminosity

For luminosities of the order of $10^{33}\mathrm{cm}^{-2}\mathrm{s}^{-1}$ two types of the first level muon trigger are considered:

1. **Inclusive single muon trigger**, $|\eta| < 2.4$, $p_t^{cut} \approx 7 - 10$ GeV
   e.g. for study of the B$\rightarrow \pi\pi$ by triggering on the muon from decay of the second b.
2. **Inclusive double muon trigger**, $|\eta| < 2.4$, $p_t^{cut} \approx 2 - 5$ GeV
   to find events where both b quarks decay into muons or to recognize two muon decays e.g. of J/ψ.

2.2 High luminosity

In case of high luminosities ($10^{34}\mathrm{cm}^{-2}\mathrm{s}^{-1}$) the trigger thresholds have to be readjusted:

1. **Inclusive single muon trigger**, $|\eta| < 2$, $p_t^{cut} \approx 25 - 100$ GeV
   to study large p_t W physics and search for massive W'.
2. **Inclusive double muon trigger**, $|\eta| < 2.5$, $p_t^{cut} \approx 10$ GeV
   this is in fact a Z^0 trigger

2.3 Different trigger systems

A large uncertainty in the estimation of physics rates, background and noise level, as well as the possibility of surprises due to "new physics" forces us to make the trigger system very flexible with a large safety margin. Therefore we envisage a possibility of having two independent muon trigger systems: one based on the muon chambers like DTBX, WLDC and CSC (see CMS LOI [1] for details), and a second one using dedicated fast detectors like RPC. Relatively low cost of the muon trigger ($\approx 2\%$ of the total CMS cost) in comparison to its importance justify such considerations.

In this paper we present results assuming RPCs as the trigger detectors, but the major part of the results is valid for the other solutions as well.

3 Principle of operation

3.1 Track bending in the magnetic field

The magnetic field in the CMS detector is created by a long superconducting solenoid (Fig. 1). Since there is no tangential ($r\varphi$) component of the **B** field, tracks are primarily bent in the $r\varphi$ plane (perpendicular to the beam direction). Thus, tracks in rz projection are approximately straight lines, i.e. they keep almost constant η value along the path. The presence of a radial field component $\mathbf{B}_r$, especially in the forward part of the detector, slightly modifies this picture. A track bent by the $\mathbf{p}_t \times \mathbf{B}$ force gets some tangential component $p_{r\varphi}$. Then $\mathbf{p}_{r\varphi} \times \mathbf{B}_r$ produce a z directed force. An effect of this force is a change of η along the path. This deflection in η is rather small because the $p_{r\varphi}$ component is small in comparison to the total p value. Even for the softest tracks reaching the muon stations the change does not exceed 0.15 (see Fig. 2). Thus, in order to measure the transverse momentum of the

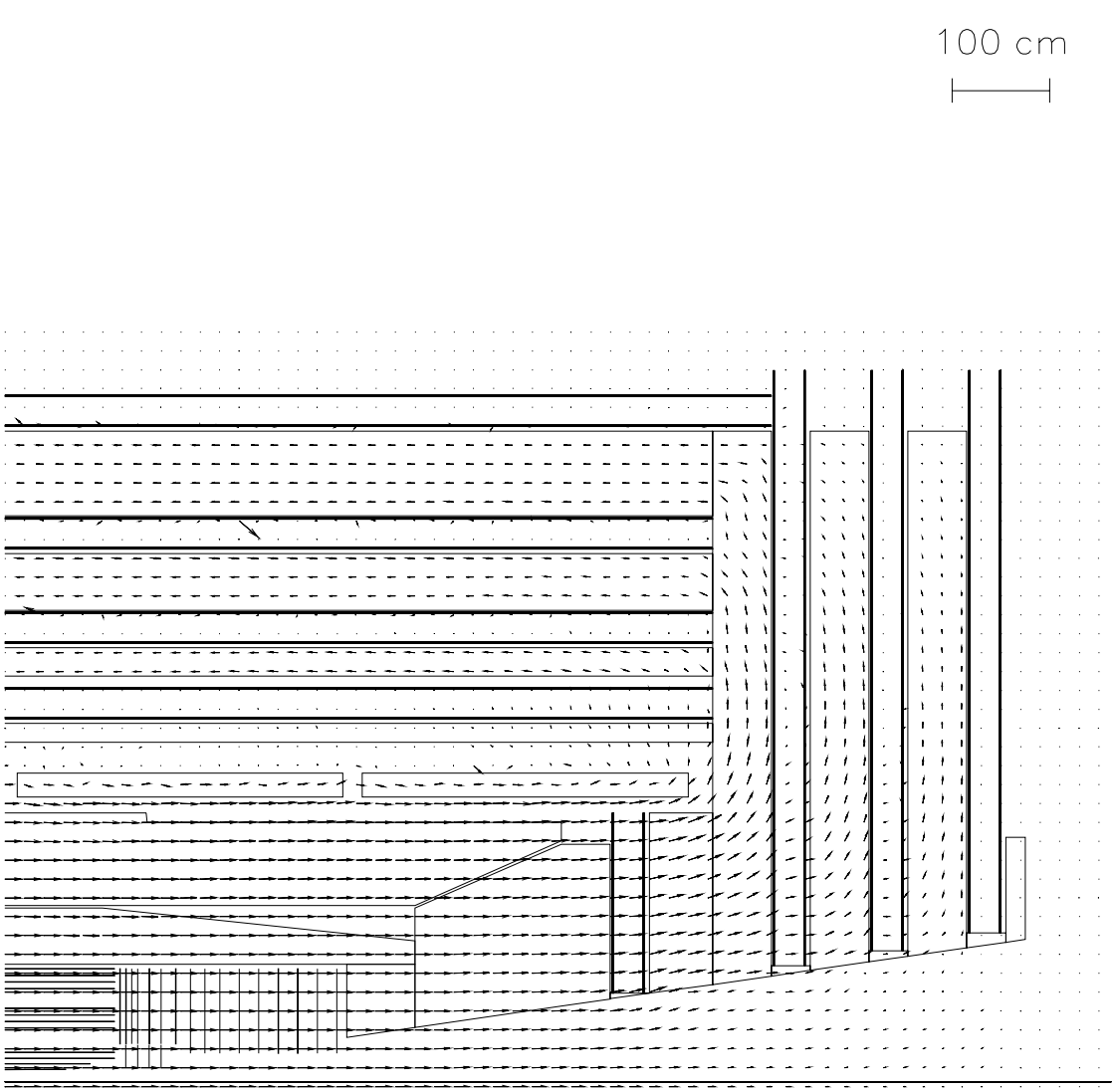

Figure 1: Magnetic field map of CMS

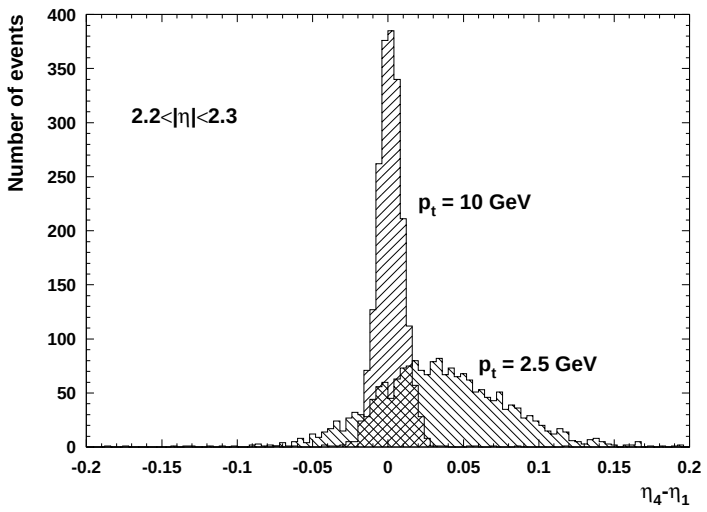

Figure 2: Track deflection in η between stations MF1 and MF4

track it is enough to observe the dominant bending in the $r\varphi$ plane. A few examples of simulated muon tracks are shown in Fig. 3.

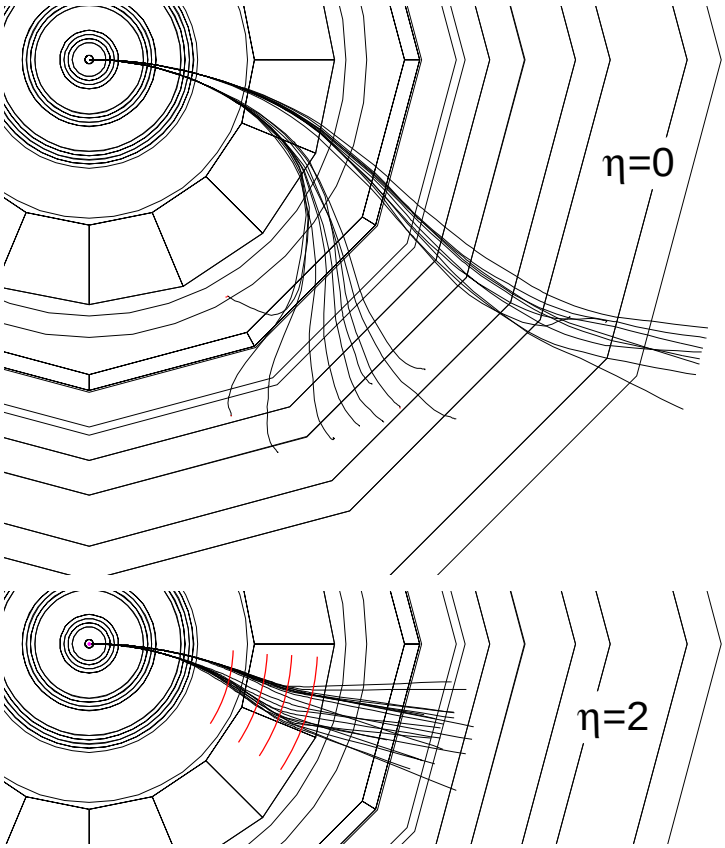

Figure 3: Simulated muon tracks with $p_t = 4$ and 6 GeV. In the second figure the places where the tracks cross the forward muon stations are indicated by four arcs.

Bending angle of the track is given by the integral of the $\mathbf{B}\times\mathbf{dl}$ product, where $\mathbf{dl}$ is an infinitesimal vector along the track. Fig. 4 shows this value as a function of R in the barrel, and as a function of Z in the forward part of the CMS detector. It grows linearly until the track reaches the coil and then it falls down in the return yoke due to the change of the sign of $\mathbf{B}\times\mathbf{dl}$.

Knowing the place where the change occurs one can make use of the whole integrated absolute value of the $\mathbf{B}\times\mathbf{dl}$ product. This value is shown in the right part of Fig. 4. One can see that in the barrel it is almost constant and approximately equal to 17 Tm. In the forward region it decreases with pseudorapidity η but even at the edge of the acceptance of the muon system it remains as large as 6 Tm. Such a big value causes the track bending to be larger then multiple scattering effect and thus allows to disentangle various momenta even for the highest η and the lowest p_t values with the acceptance of the muon system (see Fig. 5).

3.2 Triggering with patterns of hits

In principle, knowing the vertex, two measuring planes after the coil giving a local track vector are enough to measure the momentum and apply a p_t cut. However in order to deal with fluctuations due to multiple scattering and energy losses we take advantage of having 4 muon stations and make use of 4 measuring planes (one per station). A four point pattern is more redundant than the simple vector and gives a sharper cut.

The above idea has to be slightly modified for muons with $p_t < 8$ GeV in the barrel because they are not able to reach outer muon stations. Therefore we place two triggering planes in the first and the second muon station and again use a four point pattern to make the p_t cut.

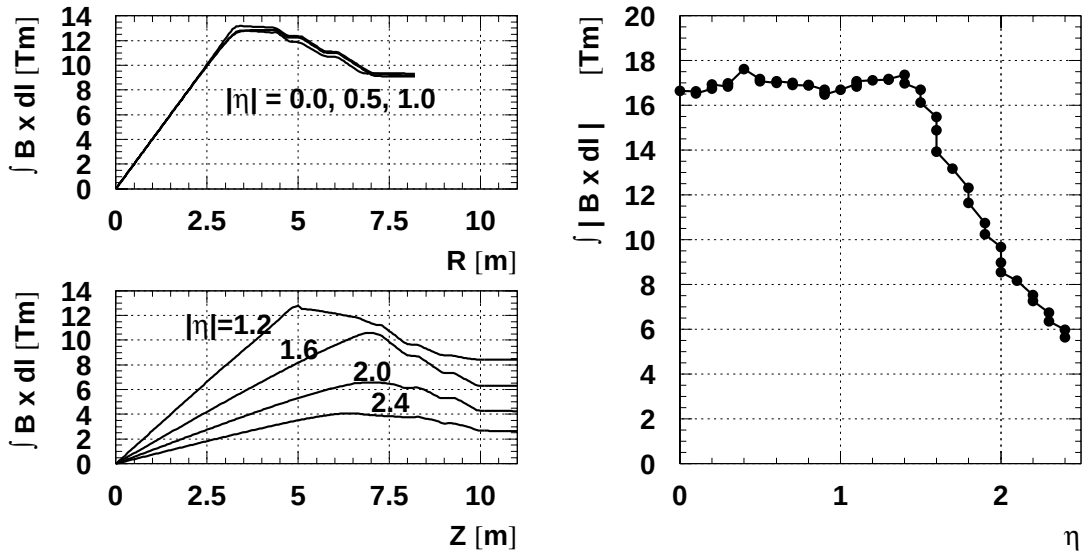

Figure 4: CMS bending power

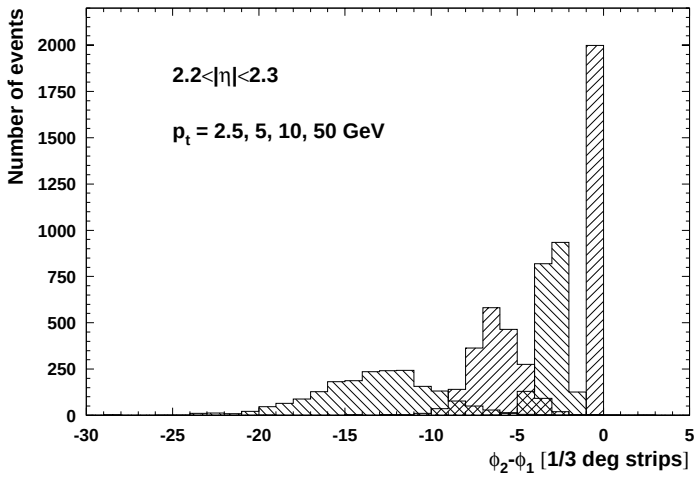

Figure 5: Track bending measured by stations MF1 and MF2

3.3 Geometry

The symmetry of the problem naturally suggests a projective geometry, both in η and φ. Since the track is bent mainly in the plane perpendicular to the beam it is enough to know precisely only the φ coordinate. Thus a measurement can be done with long strips positioned along the beam in the barrel and radially in the forward region. However, since the bending power in the forward region decreases with η some coarse knowledge of r is necessary and the strips cannot be too long.

3.4 Size of the strips

The size of the strips is determined by the following factors:

- width
  - track bending (required momentum resolution)
  - multiple scattering and energy losses
  - cluster size
- length
  - signal propagation time (bunch crossing assignment)
  - change of the bending with η
  - change of η due to the non-$r\varphi$ bending
- area (number of strips)
  - number of channels (cost)
  - complexity of the trigger processor (feasibility)
  - capacitance
  - occupancy
  - mechanics of the chambers

Taking all this into account it seems that the strip width of 1/3 degree and the length of about 0.1 η unit is a good compromise. The impact of the segmentation in φ one can see in Fig. 5 where the bending measured by the first two muon stations is shown in units of 1/3 deg wide strips. In the chapter devoted to the simulation results we will show that taking into account full pattern of hits with the given segmentation one can provide a relatively sharp p_t cut up to about 100 GeV.

Concerning the strip length the main constraint comes from the fact that a given p_t cut has to be performed by different sets of patterns for different η regions. Fig. 6 shows that the shift in $\Delta\varphi$ within an η interval of 0.1 is substantially smaller than the smearing due to multiple scattering. On the other hand it has been shown in Fig. 2 that the change of η due to the non-$r\varphi$ bending is smaller than 0.15 and thus it is enough to consider only neighboring strips.

A few examples of physical strip dimensions are given in the table below. More details on segmentation will be given in the chapter devoted to the trigger processor.

station	$\lvert\eta\rvert$	length	min. width	max. width
MS1	-0.07 – 0.07	540 mm	22 mm	22 mm
MS2	-0.07 – 0.07	595 mm	25 mm	25 mm
MS3	-0.07 – 0.07	790 mm	33 mm	33 mm
MS4	-0.07 – 0.07	970 mm	40 mm	40 mm
MF1	2.30 – 2.40	122 mm	6 mm	7 mm
MF4	2.30 – 2.40	154 mm	8 mm	9 mm

One can see from the table that the proposed geometry leads to rather small strips in the very forward region. It is technically difficult and it should be understood as a kind of feasibility limit. Before we make a final choice of the segmentation we have to study carefully what is the impact of a given design on the trigger performance in respect to the interesting physics channels. For example we can give up single muon triggering for $|\eta| > 2$ and relax the granularity in this region still keeping the double muon rate on the safe side. Extensive simulation work on this subject is going on and we hope it will converge to the final decision before the Technical Proposal release.

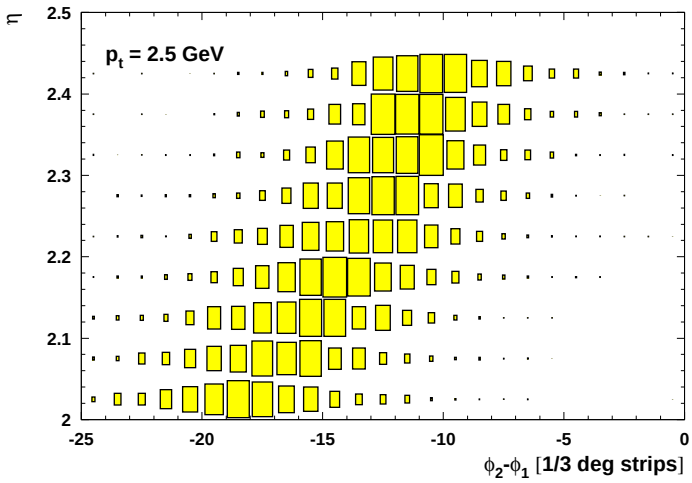

Figure 6: Track bending for various η.

3.5 Parallel Plate Chamber version geometry

In case of Parallel Plate Chambers it is more difficult to arrange fully projective geometry. In principle one can produce PPC of any shape, but large number of shapes needed for a projective geometry substantially increases the cost. Therefore it seems to be more feasible to build triggering planes with rectangular PPCs, e.g. 5×5 cm^2 equipped with 6-10 mm strips. In this case the overall idea of triggering on hit patterns remains unchanged. Only the algorithm of preparing sets of valid patterns becomes more complicated, because we can not directly use symmetry in φ. Each segment trigger processor (see next chapter) has to have programmed different sets of patterns. Such a possibility we have foreseen even for the φ-symmetric version in order to deal with geometrical inefficiencies and local hardware problems like dead and noisy channels etc.

4 Resistive Plate Chambers

Severe timing condition at LHC requires fast triggering detectors. In case of muon trigger the Resistive Plate Chambers (RPC) are very attractive candidates [2]. The only drawback of the RPCs is the limited rate capability. Standard RPC can stand up to $\approx$ 100 Hz/cm^2 without a significant loss in efficiency. In the region above $|\eta| = 2$ the particle rate can exceed this value and therefore the Parallel Plate Chambers (PPC) [1, 3], have been foreseen to cover this region. However recent encouraging results with pure Freon RPCs [4] give a hope that the RPC technique can be used in this η region.

4.1 The Warsaw RPC Prototype

A prototype RPC chamber was constructed in Warsaw in spring '93. It was first tested with radioactive iron source and with cosmic ray telescope in Warsaw and subsequently brought to CERN for test in the RD5 beam. We used the same gas composition as other RPCs: 58.2% Ar, 38.0% n-butane and 3.8% freon. The chamber size is 50×50 cm^2 and the strips are 1 cm wide. The plane specific resistivity is about 10^{12} Ω×cm. Twelve strips were read out with a LeCroy ADC. Their OR-ed signal was read with a TDC. Data were taken with various HV values and beam intensities. A typical spectrum of the sum of ADC channels is shown in Fig. 7 a. The chamber efficiency is defined as a ratio of the number of events with the sum above 100 ADC counts to the number of events taken.

In the Fig. 7 b the chamber efficiency as a function of high voltage is shown for the incoming rate of about 10 Hz/cm^2. The chamber noise dependence on high voltage is shown in Fig. 7 c. Fig. 7 d shows the chamber efficiency versus incoming rate. The chamber behavior during the spill can be seen in the Fig. 8 a and b, which show the average sum of ADCs and efficiency as a function of time. For the beam tracks rate about 23 Hz/cm^2 the average sum falls by 50% and efficiency by about 20%. When the rate reaches to 370 Hz/cm^2 the efficiency drop is much more dramatic - it falls to about 10%. The TDC spectrum is shown in Fig. 8 c. Its spread is about 7 nanoseconds. The average multiplicity of

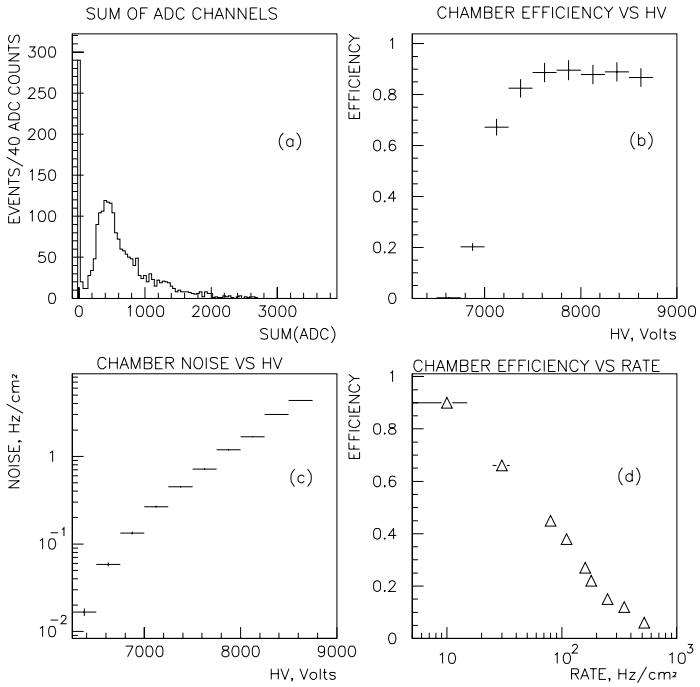

Figure 7: Results of Warsaw RPC prototypes tests in RD5

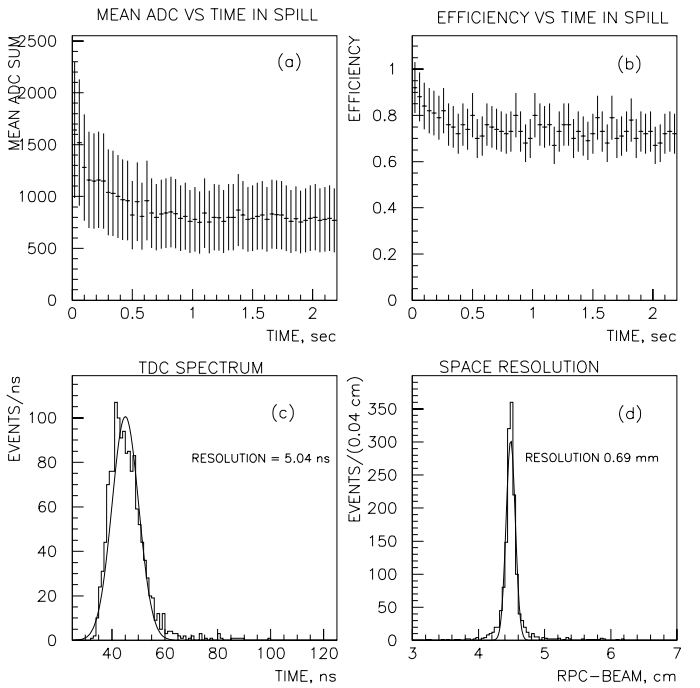

Figure 8: Results of Warsaw RPC prototypes tests in RD5

strips with ADC value above pedestal is about 3.5 corresponding to the avalanche size of 3.5 cm. The space resolution of the chamber was obtained by comparing the center of gravity of ADC signals with track position known from the beam reconstruction. The resolution is below 1 mm, as can be seen from Fig. 8 d.

The above results can be compared with the results of the Rome Group of RD5 [2]:

parameter	Warsaw	Rome		unit
resistivity	10^{12}	10^{11}	$4 \cdot 10^{10}$	$\Omega\times$cm
operating HV	8250	7200	7000	V
noise	2.0	0.1	0.5	Hz/cm^2
critical rate ($\varepsilon = 80\%$)	20	50	200	Hz/cm^2
average cluster size	3.5	4.0	8.7	cm
time resolution (σ)	5	1.8 – 4.4		ns

Performance differences can be partially explained by different resistivity. In fact the Warsaw chamber plates were ordered and delivered with resistivity 10^{11} $\Omega\times$cm, but it rose up to 10^{12} $\Omega\times$cm during one month preceding the tests in RD5. This fact points to the necessity of long term studies on material ageing.

The larger noise of the Warsaw prototype is caused by higher operating HV. The noise rates of the Rome and Warsaw RPCS measured at the same HV are comparable.

The critical difference in dependence of efficiency on the rate comes mainly from different resistivities, however one should keep in mind that the second Rome prototype is a double gap RPC. It is also very important that quoted efficiency is in fact an average over the 2.6 s accelerator period because the efficiency falls down with time. In case of the Warsaw RPC it saturates after about 0.7 s and the observed plateau reflects the situation expected in a DC machine (LHC is practically the case). In case of Rome prototypes there is no sign of approaching the plateau during the whole 2.6 s cycle and thus one cannot predict efficiency at DC operating mode. In order to get a reliable number the measurement has to be done with longer illumination periods.

Variation of the cluster size with the resistivity opposite to the variation of the efficiency indicates that there is some tradeoff between the two variables. It maybe difficult to obtain small clusters and high efficiency at the same time.

Finally the time resolution is for all prototypes of the order of a few nanoseconds, although depends on the illumination rate. Another related problem is that also the average answer time changes with rate as much as a few nanoseconds.

A conclusion from all these studies is that we understand better operating of the RPCs but the optimization process should go on. First of all we would like to improve the chamber efficiency and the rate capability, minimize the response time uncertainty and reduce the cluster size.

5 Trigger processor

5.1 The algorithm

5.1.1 Basic principle

A particle passing the detector crosses muon stations, hitting the detector strips on its way. In the absence of the energy loss and multiple scattering there will be a one to one correspondence between the pattern of hits and the muon transverse momentum. In the real world with energy loss and multiple scattering there is a set of hit patterns for each value of p_t. The sets of valid patterns change with pseudorapidity η. They are practically η independent in the barrel region, but vary in the forward region. The sets of patterns for various transverse momenta are ordered i.e. a higher p_t set is a subset of a lower p_t set. This property allows us to establish the set of patterns for a given value of the threshold p_t^{cut}. Such a set can be loaded into a trigger processor. Then every observed track pattern is compared with the predefined patterns. A track gives a trigger if its pattern belongs to the set of valid patterns.

5.1.2 Dead areas and detector inefficiencies

Insensitive areas of each triggering plane are distributed in such a way that ≈90% of tracks cross 4 planes, ≈9% – 3 planes, and remaining 1% – two planes only. Tracks crossing 3 planes are recovered by a modified trigger algorithm. Hit patterns are checked assuming that there was a hit in a dead region of a missing plane. Two hit tracks are not recovered to avoid encountering random hits from any source. In order to take into account this loss as well as some intrinsic detector inefficiency, we assume a global inefficiency of the muon trigger to be equal to 5%.

5.1.3 Clustering

Large multiple scattering and energy losses at low momenta cause large fluctuations of track shapes. It leads to a rapid increase of the number of valid patterns. On the other hand low p_t tracks are more bent and high granularity of the detectors is not needed. Taking this into account one can reduce the number of patterns to be fed into processor by OR'ing a few neighboring strips. In other words the logical strip size can be increased. First such an algorithm has been already successfully implemented into the ALTERA 7128 chip. One 25 ns step (LHC bunch crossing distance) is enough to perform this task.

5.1.4 Declustering

Opposite problems occur in high p_t region. There multiple scattering and energy losses can be neglected, but tracks are rather straight and it is difficult to distinguish say, 50 and 100 GeV tracks. The situation is even more complicated by the fact that sometimes two or more neighboring strips are fired. One way to improve is reducing the cluster size. This possibility can be however limited by the tradeoff with efficiency. Another way is to implement a trigger algorithm which is able to deal with cluster. The simplest algorithm one can think of duplicates the number of logical strips. Single hit physical strips correspond to even logical strips. If two physical strips are fired then the corresponding odd strip is set on. In case of tree strips fired the even logical strip assigned to the middle of the tippled is set on etc. We plan to study performance and feasibility of similar algorithms in the near future.

5.2 Segmentation

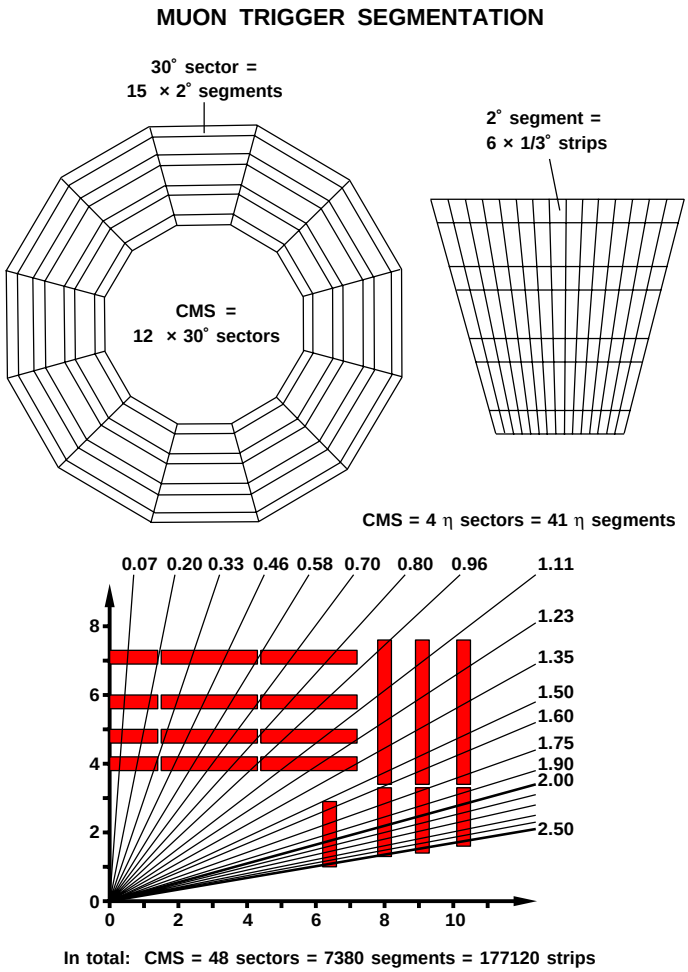

Figure 9: Muon trigger segmentation.

An information from all triggering planes within a certain region of the detector is first processed locally by so called segment trigger processor. At the moment the segment is assumed to be 1 strip long and 6 strips wide and thus it covers 2 degrees in φ and ≈ 0.1 η unit. These numbers determine double

muon resolution of the trigger, i.e. two muon within the same segment will be seen as only one. Therefore they are still a subject of optimization and an impact of the choice will be studied with a simulation of interesting physics channels.

Segments are arranged in larger units called sectors as shown in Fig. 9. Detailed functionality of segment and sector processors is described in the following chapters.

5.3 Trigger processor components

Electronic instrumentation of the MTS (RPC) system consist of:

- front-end analog electronics,
- segment trigger and readout module (STRM),
- sector trigger module (STM),
- high voltage system,
- low voltage and gas monitoring system

They will be supported by other modules - parts of different CMS utilities :

- timing distribution network,
- front-end bus as a connection to the CMS data acquisition scheme.

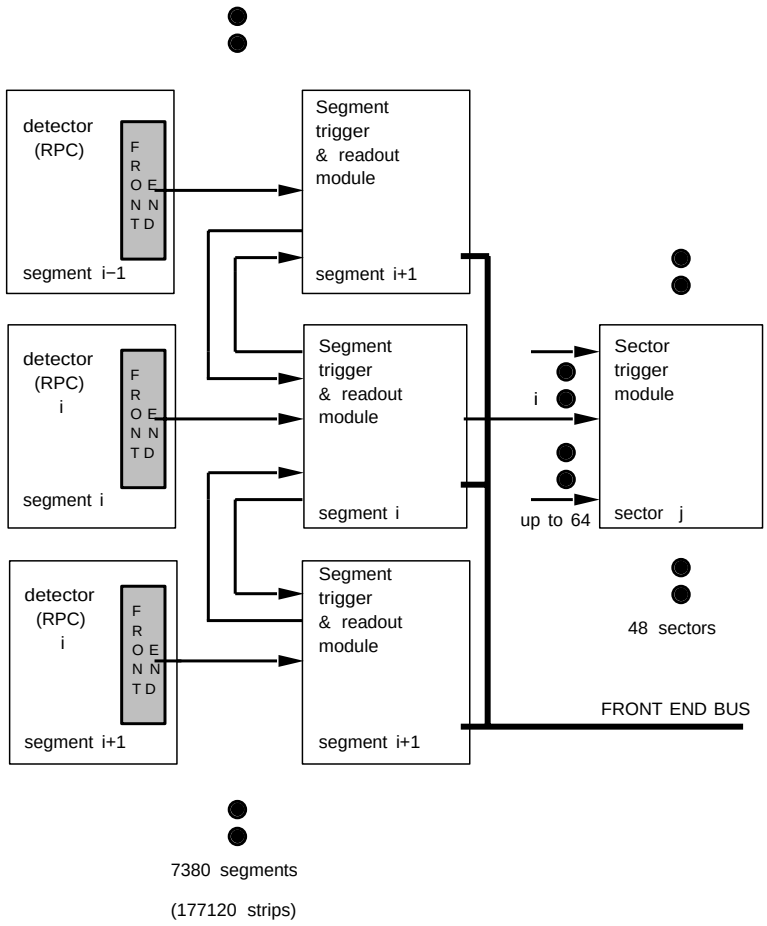

Figure 10: General schematic of muon trigger.

We propose to locate most of our electronics on the detector to avoid long connections and additional timing compensations needed due to them. Only very reduced data stream will come out of our segment and sector electronics placed on the detector. However, special care will be needed to make this electronics

error free and fully testable.This task will be simplified by the fact that the main part of our electronics will be programable.

All elements of our electronics in subdetector data stream will have pipelined structure, that is the MTS system will provide information for each bunch crossing so there will be no dead time in our system.

5.4 Front-end analog electronics

Aim of this part of electronics is to provide low jitter digital signals which could be transmitted over the distance of about 10 meters into the STRM without signal quality degradation. RPC's provide high amplitude, fast signal with the time resolution of about 5 ns so relatively simple discriminator will be needed. The choice of the discriminator will have to wait till more is known about final RPC pulse shape and amplitude. We plan to equip our front-end electronics with calibration facility which will be controlled from STRM.

5.5 Segment trigger and readout module

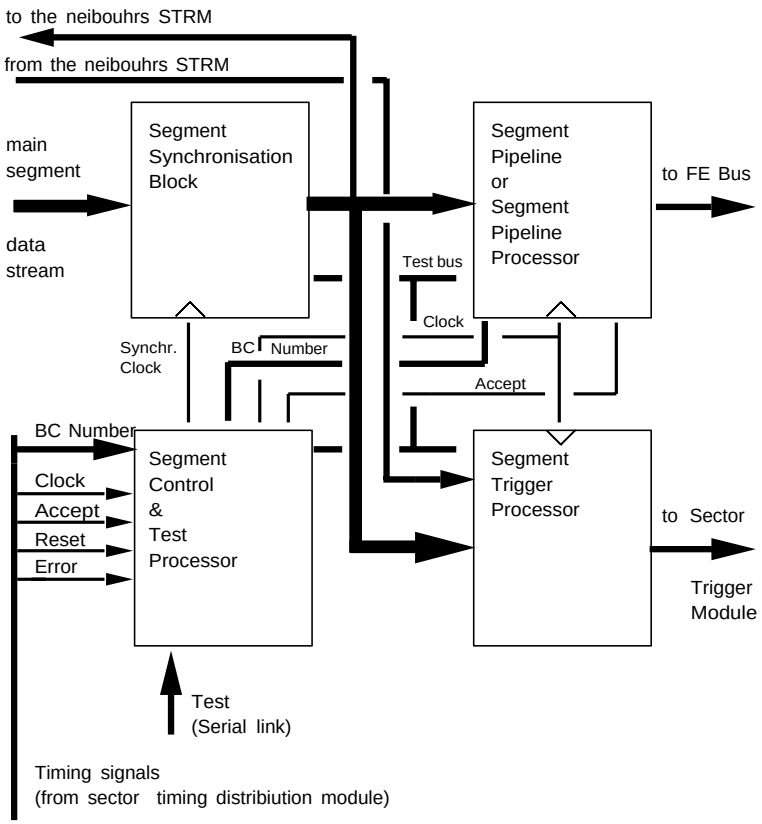

Figure 11: Segment trigger and readout module.

STRM will consist of four blocks:

- synchronisation block,
- control and test processor,
- pipeline processor,
- trigger processor.

5.5.1 Segment synchronisation block

The purpose of the synchronisation block will be to synchronise the signals coming from 4 different muon stations and to provide signals related to only one specific bunch crossing. Since low momentum muons frequently cross segment boundaries, certain part of the synchronised signals will be sent to the neighboring STRMs. We envisage also a possibility to inhibit a channel which has registered a signal for

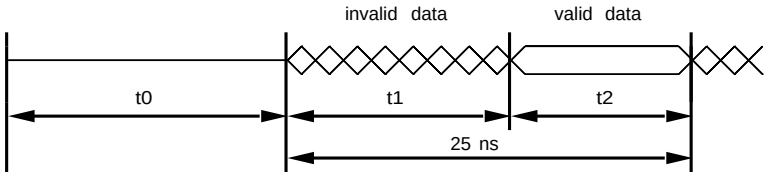

t0 = time of flight to the strip
+ detector delay
+ front_end_electronics delay
+ cable delay
+ synchronisation logic setup time

t1= detector response uncertainity (geometry, signal time resolution)
+ front_end_electronics jitter
+cable delay jitter

t2= 25 ns − t1

Figure 12: Synchronisation block.

programmable amount of crossings to avoid afterpulses. This is allowed by very low particle rate in our subdetector.

The elements providing the synchronisation will be located in this block but control will come from control processor. To make this synchronisation possible very precise timing model of segment is necessary. Work on this has already started. This model will define the total delay and jitter of the signals for each station (the signals coming out of one station will have the same timing properties). Model has to determine:

- particle time of flight from the vertex to the strip,
- detector delay (including signal propagation along strip),
- front end electronics delay and jitter,
- cable delay.

Final version of this model (containing the electronics location) will determine cable lengths needed for connecting chambers within a given segment and data needed to perform the synchronisation task.

5.5.2 Segment control and test processor

Control and test processor will serve as the interface to the timing distribution module and will provide the different clocks for STRM elements. The number of timing distribution modules for MTS (RPC) will be the same as the number of sectors, that is 48. Control and test processor will provide an interface to serial link used for downloading data to the programmable parts of segment module and to control execution of internal test procedures which will be incorporated into segment module. These functions could be based on IEEE 1149.1 JTAG standard. It will allow us to establish the status of the segment module electronics and to reprogram the module if faulty behavior of detector elements dictates so. The task of detector calibration will be also controlled from this unit.

5.5.3 Segment pipeline processor

Pipeline processor will

- store the data during the time when first level trigger decision (Accept signal) is elaborated (pipeline memory),
- store the data corresponding to the bunch crossing accepted by first level trigger (derandomizer buffer),
- serve as interface to the CMS data acquisition scheme.

We could use synchronous or asynchronous procedure. In each case data coming out of STRM will be supplied with corresponding bunch crossing number. We do not plan to build our own pipeline chip – there exist projects to build this pipeline memory. The cost and facility of interfacing will decide which one we will use.

5.5.4 Segment trigger processor

This is the main part of our segment module. The purpose of this processor is to provide the information about the highest momentum muon passing through the segment area. The output of the processor will be a 3-bit code of the muon momentum. Code "0" means that there was no muon in the segment (or that its momentum was below the lowest threshold). Segment processor will use as its input data from segment synchronisation processor as well as the synchronised data coming into segment from neighbor STRM. In this case additional resynchronisation will be needed. Segment trigger processor will contain the pattern recognition part and the momentum cut definition part. The first part consists of 4 inputs (one for each muon plane) and gates containing the patterns. Each pattern defines one accepted muon track found in four muon stations. The other part will perform the grouping of the and gates outputs and will store them in the 3-bit encoder unit. Some additional data treatment will be needed in the input stage to declusterize the muon station data and to resolve the chamber inefficiency problem. All this operation we would like to perform in a programmable device, to have a possibility to change the track patterns, coding, declustering and inefficiency resolving algorithms as needed. There is also a possibility to group strips in pseudostrips (by or-ing them) to cope with growing number of patterns for low momentum muons. By a pattern we mean a set of positions of hits in muon stations 2, 3, 4 in relation to the station 1. Patterns will be given by the simulation of the muon tracks in the detector and of the detector response. The information about dead or noisy strips will be also included in the patterns. The trigger processor will operate in pipelined mode, therefore there will be no dead time. The downloading of the trigger processor will be performed by the control processor through the serial link. We have already tested the use of some of programmable devices existing on the market. The result are very encouraging. For example ALTERA 7128 (about 4000 available gates) can contain up to about 300 different track patterns. Trigger algorithm is executed in two 25 ns clock periods with sufficient margin. ALTERA 7000 series EPLD has no downloading facility, but other devices which have this possibility are coming. It is also possible to build a special ASIC which will be programmable and will be specially dedicated to this application.

5.6 Sector trigger processor

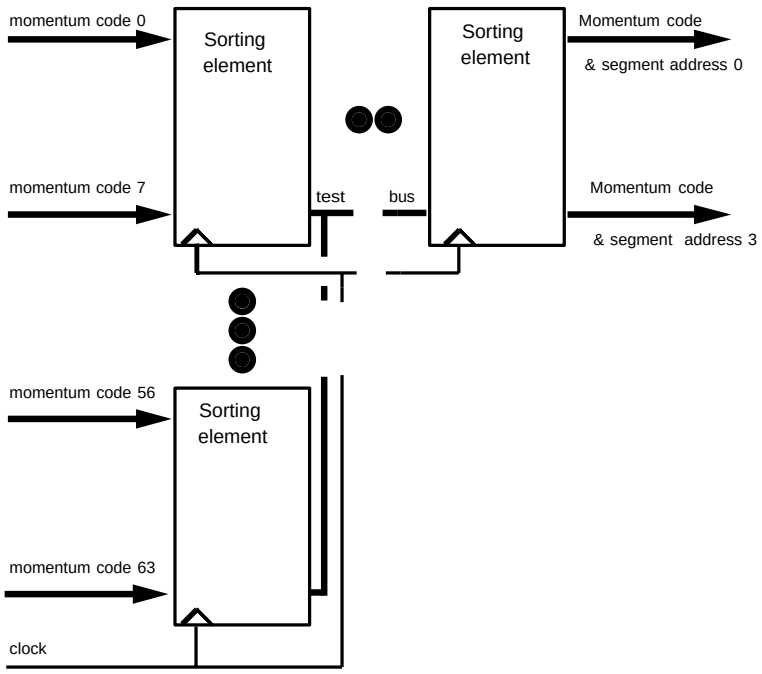

Figure 13: Sector trigger module.

The sector trigger processor will find up to four highest momentum muons in a sector area. The codes of momentum cuts as well as corresponding addresses of segments will be given. The structure of the sector processor will be distributed, that means that the different parts of the STM will be located in different places.The reason is to minimize the length of the cables. This part of the MTS system was already tested using programmable devices. Results show that even with today's electronics the algorithm for STM could be realized in 12 clock periods of 25 ns. Expecting that faster and bigger devices will be accessible in the future this decision could be done in about 8×25 ns.

5.7 Beam tests in RD5

The first Trigger Processor (TP) prototype has been already constructed. It was a segment processor programmed for high momentum muons. It has been tested in lab and then in the RD5 experiment during the August/September run. The aim of the test was to check the feasibility of the design and its ability to run with high speed. Three programmable ALTERA 7128 chips were used in the TP and housed in a VME module (see Fig. 14).

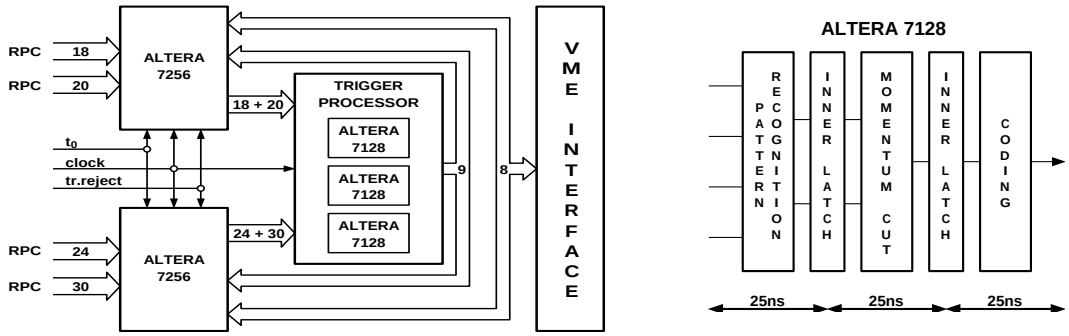

Figure 14: Schematic of the trigger processor board and segment processor chip.

The TP uses information from the RPC's, which are part of the RD5 setup. The chambers are placed in a field of two magnets (1.5 and 3 T) simulating the magnetic field of CMS. Four chambers with horizontal strips were selected and their digital outputs were fed into the TP. The decision taking of the TP is based on patterns of hits which were chosen using data from previous RD5 runs. Six groups of patterns are used corresponding to momentum thresholds of 10, 20, 30, 50, 75 and 100 GeV. The seventh group corresponds to straight tracks (marked as "1000 GeV"). The TP responds with the pattern group number or with zero if no match is found in an event. In case where several matching patterns are found in the event (due to many strips having fired in some chambers) the group number corresponding to maximal momentum is output.

The TP processes data continously with a supplied clock. It reads data from the RPC's and processes them during 4 clock ticks. When the RD5 tiggering signal arrives the data are read by the Data Acquisition computers. The clock period of 60 ns has been used in this test but the module was earlier tested in lab with a 25 ns clock corresponding to the time interval between consecutive beam crossings of the LHC.

Due to lack of beam time we took data with only four beam energies: 20, 30, 50 and 100 GeV. Fig. 15 shows the trigger efficiency as a function of the beam energy for different thresholds. In offline analysis it was checked that the TP response is in agreement with what we expect it to be from the direct readout of the RPC strips. This agreement is obtained in 100% of events.

We attribute the fact that the trigger efficiency as a function of the beam energy is not a very steep one to the cluster size in the RPC's. It is confirmed in Fig. 16, where we show the trigger efficiency for the threshold value of 30 GeV but with different requirements on strip multiplicities. First we show all data, then ask for multiplicities in all chamber not to be larger than 4, then 3, then 2 and finally ask for multiplicities of 1-2-2-2 and 1-1-2-2 in the last plot.

The current version of the TP requires signals from all four chambers to give an answer. During the next year running we plan to include patterns corresponding to cases, when one of the chambers is missing thus increasing the TP efficiency.

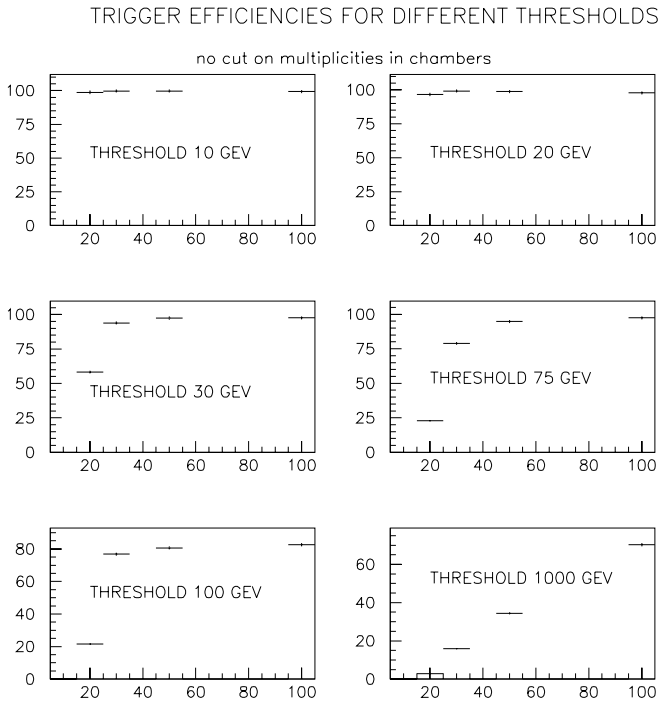

Figure 15: Trigger efficiency as a function of the beam energy for p_t^{cut} = 10, 20, 30, 75, 100 and 1000 GeV.

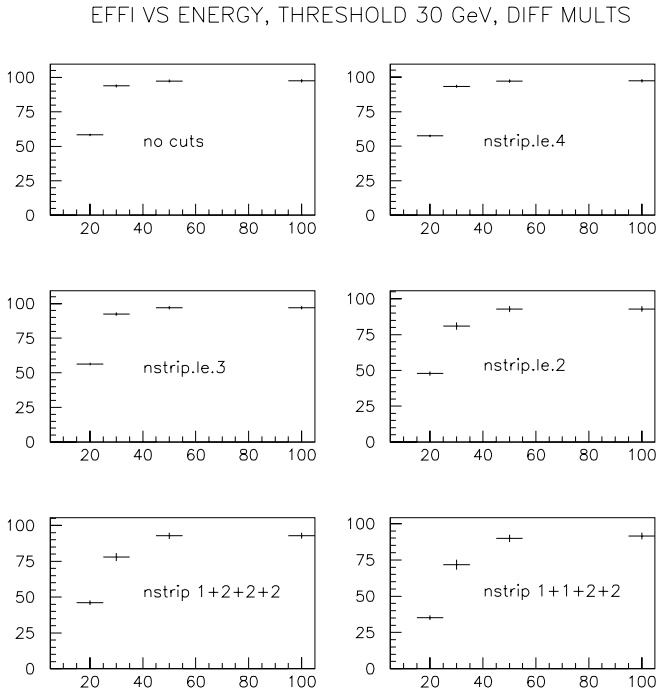

Figure 16: Trigger efficiency for a 30 GeV threshold for different multiplicities.

6 Simulation study

6.1 Efficiency curves

The presented trigger algorithm has been applied to simulated data in order to calculate efficiency curves and final trigger rates [5]. The CMS simulation program CMSIM [6] based on the GEANT package has been used to track muons with p_t between 0.5 and 100 GeV through the CMS detector. In total $\approx 10^7$ events have been simulated. Multiple scattering, energy loss and production of secondaries have been taken into account. The obtained efficiency curves as a function of the muon p_t for different values of p_t^{cut} and η are shown in Fig. 17.

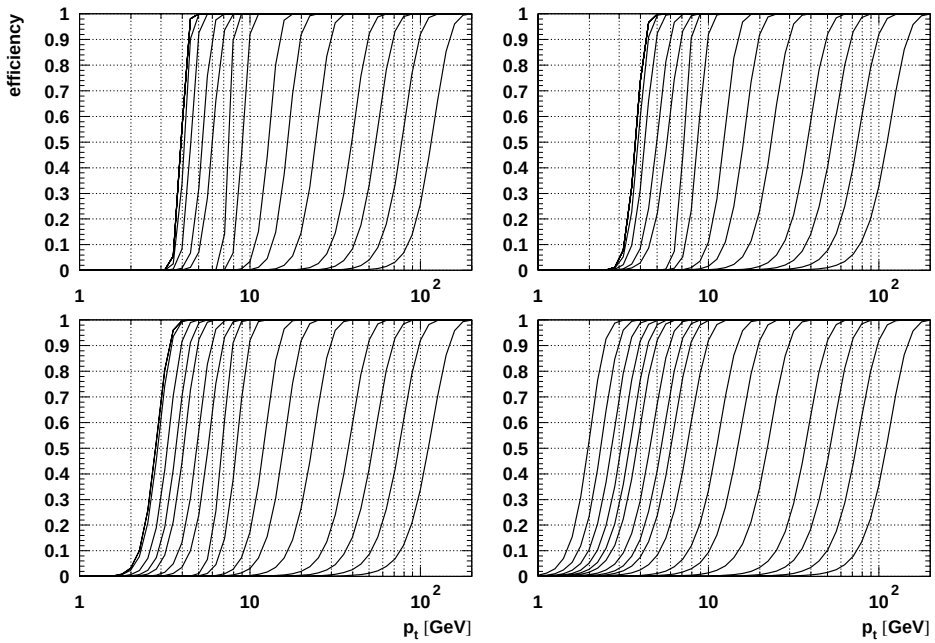

Figure 17: Muon trigger efficiency curves for four $|\eta|$ regions: 0-0.8, 0.8-1.5, 1.5-2.0 and 2.0-2.5 respectively.

The efficiency curves have been then parametrized as a function of the p_t^{cut} value, and p_t and η of a particle, to be used further in the physics analysis.

6.2 Estimation of rates

In order to estimate trigger rates 10^6, minimum bias events have been generated with PYTHIA. PYTHIA parameters have been tuned to reproduce UA1 data and then extrapolated to LHC energy. The Peterson fragmentation function has been chosen. It has been checked that this sample contains 0.65% bb pairs, which is close to what one can expect: σ(bb) / σ(total inelastic) $\approx$ 500 μb / 100 mb for minimum bias collisions at $\sqrt{s}$ = 14 TeV.

In addition, about 10^6 two-jet events with $p_t^{jet} > 20$ and 40 GeV have been generated in order to increase statistics of high p_t events. Spectra of muons and hadrons from this sample have been parametrized and then convoluted with the efficiency curves. Starting from the inclusive hadron spectrum we have estimated the rate due to punchthrough using GEISHA shower simulation. This has been checked against measurements made in the RD5 experiment [7].

In the case of the minimum bias sample, entire events have been fed into the CMSIM/GEANT simulation and the trigger algorithm has been applied to all the particles. Good agreement of results in the overlap region of the two samples allows us to predict trigger rates in a wide range of possible p_t thresholds. The resulting integrated trigger rates for various p_t^{cut} values at the luminosity 10^{33} cm^{-2}s^{-1} are shown in Fig. 18. The rates approximately scale with the luminosity because pileup effects do not play an important role.

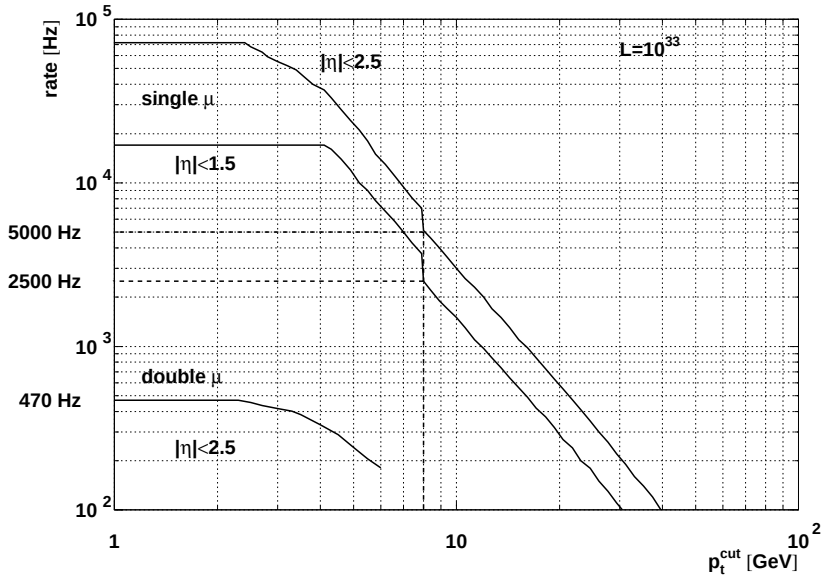

Figure 18: First level muon trigger rates.

6.3 Discussion of results

6.3.1 Trigger thresholds for physics analysis

Since the high luminosity trigger has been already discussed in the LOI [1] here we concentrate on the low luminosity case. The upper limit on the first level trigger rate is given by the performance of the CMS event filter. The event filter is designed to stand 50 kHz rate at full LHC luminosity. In the first staging phase the computing power of the event filter will be significantly reduced, but on the other hand we expect much lower luminosities. This means that the amount of data per event to be analyzed will be also reduced (less pp collisions per bunch crossing) and thus the event rate acceptable for the event filter will stay approximately the same. Thus, with a large safety margin, one can assume that a few kHz rate is allowed for the first level muon trigger.

The few kHz limit brings us to a p_t threshold of the order of 7-10 GeV for single muons. Looking at the rate curves in this region, one can see a 70% jump at 8 GeV. This is due to the change of the algorithm described in Sec. 3.2. Therefore choosing the p_t^{cut} slightly below 8 GeV is not advisable because the increase in rate is bigger than the gain in acceptance. Limiting the η range also does not help very much, e.g. the change of the η limit from 2.5 to 1.5 decreases the rate only by a factor 2. Taking all this into account the optimal p_t^{cut} for the single muon trigger seems to be 8 GeV and we assume this value for further physics analysis. This value gives the trigger rate of 5 kHz.

The overall dimuon trigger rates saturate at the level below 500 Hz. It is impossible to increase further the number of accepted particles by lowering the p_t threshold, i.e. allowing more and more patterns. This is due to the limited range of particles in the calorimeter absorbers. One can see from Fig. 17 and 19 that the lowest values of the p_t^{cut} (by definition at 90% efficiency) are the following:

$$\begin{aligned} \text{for } |\eta| < 1.5&: \ 4.3 \text{ GeV} \\ 1.5 < |\eta| < 2.0&: \ 3.4 \text{ GeV} \\ 2.0 < |\eta| < 2.5&: \ 2.4 \text{ GeV} \end{aligned}$$

Since the rate of 500 Hz is well acceptable by the CMS event filter we assume p_t^{cut} values listed above for further analysis. These lower p_t limits are essentially given by the natural cut on the muon energy lost in the calorimeters. One can see it by comparing the muon system acceptance with the trigger efficiency, both presented in Fig. 19. However it does not mean that the trigger pattern recognition algorithm is not needed in this region. It rejects random coincidences of hits from any source which is especially important in the very forward region.

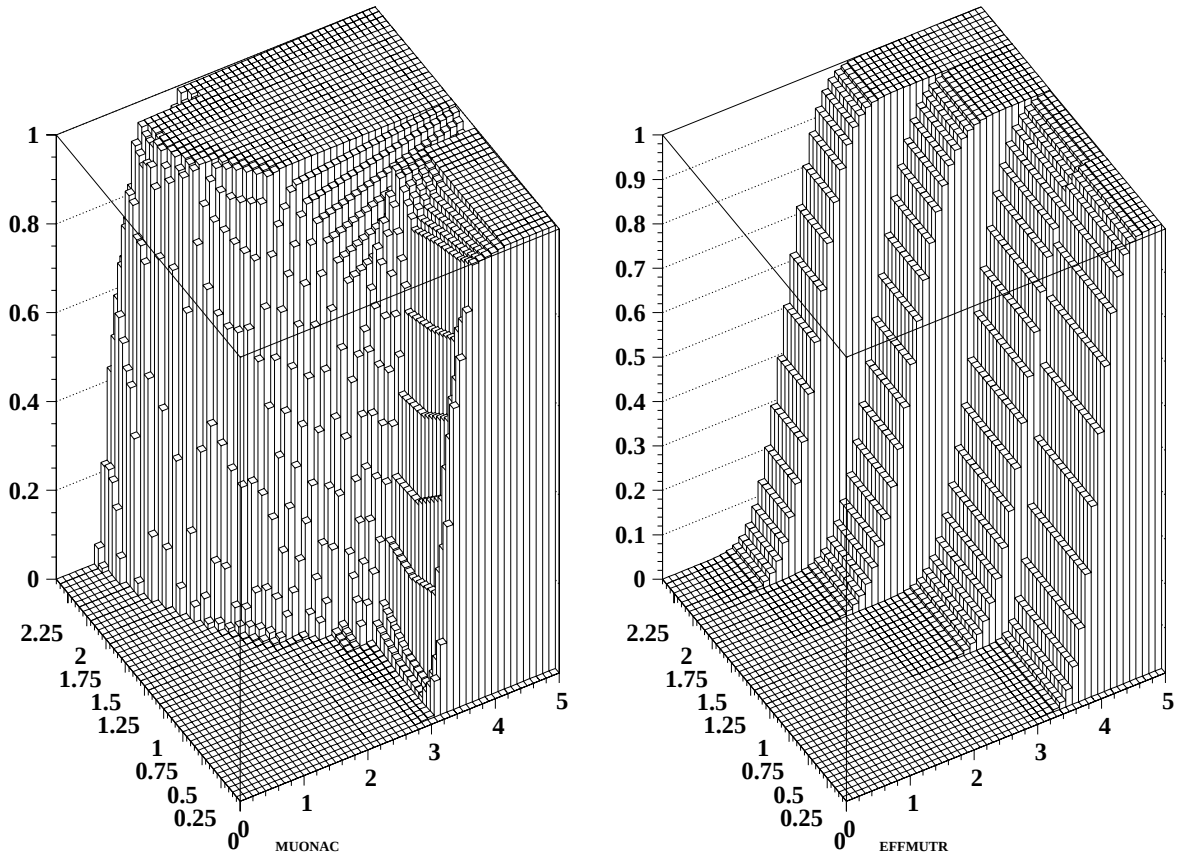

Figure 19: Acceptance of the muon system and trigger efficiency curves as a function of η (0–2.4) and p_t (0–5 GeV).

6.3.2 Future prospects

We envisage two ways of improving trigger acceptance for low p_t events. One is by applying a multilevel trigger structure in the event filter, the second one is by combining the information from the muon system and from the calorimeter already at the first trigger level.

The CMS detector does not have a hardware second level trigger. Right after the first level decision, the detector data are read into the event filter. However, a multilevel trigger structure is foreseen to be implemented into the filtering software. An example of such a second level trigger can be a fast pattern recognition algorithm looking for straight tracks in the inner tracker and applying an effective mass cut. After a negative answer an event can be immediately rejected. Such a scheme can significantly increase the first level trigger rate acceptable for the event filter, and thus it can make possible to lower the p_t threshold.

Another scheme we are going to study relies on the information from both the muon system and from the calorimeter. The information from muon and calorimeter triggers could be first processed and correlated locally, in the small segments of the detector, allowing for combining the muon p_t threshold with a calorimeter veto–isolation cut. This way a substantially reduced number of triggers would be sent to the global trigger, allowing for a lower p_t threshold. This scheme implies, however, more powerful sector trigger processors than envisaged up to now. The implications of this idea have to be more thoroughly studied in terms of timing, cost, robustness, and reliability.

Acknowledgment

Authors would like to acknowledge the support of Polish Committee for Scientific Research under grants KBN-PB-2 0422 91 01 and KBN-SPUB-206/93.

References

[1] *CMS Letter of Intent*, CERN/LHCC 92-3.

[2] R. Santonico, R. Cardarelli, Nucl. Instr. Meth. 187 (1981)377,
R. Cardarelli et.al., Nucl. Instr. Meth. A263 (1988) 20,
M. Andlinger et all., *Study of Resistive Plate Chambers for muon detection at hadron colliders*, Preprint of "La Sapienza" Rome University, n^o 1015, July 9, 1993.

[3] A. Arefiev et all., *Parallel Plate Chambers: a fast detector for ionizing particles*, submitted to Nucl. Instr. Meth.

[4] R. Cardarelli, *Test of RPC Operating with Pure CF_3Br at RD5*, talk given at the International Workshop on the Resistive Plate Chambers in Particle Physics and Astrophysics, Rome, February 18-19, 1993.

[5] M. Konecki, Warsaw University M.Sc. thesis, 1992, unpublished,
M. Konecki, J. Królikowski, G. Wrochna, *Simulation study of the single muon, RPC based trigger for CMS*, CMS TN/92-39,
A. Csilling, M. Konecki, J. Królikowski, G. Wrochna, C.-E. Wulz, *Simulation study of the low p_t, RPC based muon trigger for CMS*, CMS technical note in preparation.

[6] C. Charlot, V. Genchev, V. Karimäki, M. Pimiä, P. Moissenz, A. Rosowsky, G. Wrochna, *CMSIM-CMANA, CMS Simulation Facilities*, CMS TN/93-63.

[7] *Status Report of the RD5 Experiment*, CERN/DRDC 91-53.